HHS Public Access

Author manuscript

Biol Psychiatry. Author manuscript; available in PMC 2018 February 15.

Published in final edited form as:

Biol Psychiatry. 2017 February 15; 81(4): 366–377. doi:10.1016/j.biopsych.2015.10.026.

Connections of the mouse orbitofrontal cortex and regulation of goal-directed action selection by BDNF-TrkB

Kelsey S. Zimmermann[1,2,3,4], **John A. Yamin**[1,3], **Donald G. Rainnie**[2,3,4], **Kerry J. Ressler**[2,3,4,5], and **Shannon L. Gourley**[1,2,3,4]

[1]Department of Pediatrics, Emory University, Atlanta, GA USA

[2]Department of Psychiatry and Behavioral Sciences, Emory University, Atlanta, GA USA

[3]Yerkes National Primate Research Center, Emory University, Atlanta, GA USA

[4]Graduate Program in Neuroscience, Emory University, Atlanta, GA USA

[5]Howard Hughes Medical Institute, Bethesda, MD, USA

Abstract

Background—Distinguishing between actions that are more, or less, likely to be rewarded is a critical aspect of goal-directed decision-making. However, neuroanatomical and molecular mechanisms are not fully understood.

Methods—We used anterograde tracing, viral-mediated gene silencing, functional disconnection strategies, pharmacological rescue, and Designer Receptors Exclusively Activated by Designer Drugs (DREADDs) to determine the anatomical and functional connectivity between the orbitofrontal cortex (oPFC) and the amygdala in mice. In particular, we knocked down *Brain-derived neurotrophic factor (Bdnf)* bilaterally in the oPFC, or generated an oPFC-amygdala "disconnection" by pairing unilateral oPFC *Bdnf* knockdown with lesions of the contralateral amygdala. We characterized decision-making strategies using a task wherein mice select actions based on the likelihood that they will be reinforced. Additionally, we assessed the effects of DREADD-mediated oPFC inhibition on the consolidation of action-outcome conditioning.

Results—As in other species, the oPFC projects to the basolateral amygdala and dorsal striatum in mice. Bilateral *Bdnf* knockdown within the ventrolateral oPFC, and unilateral *Bdnf* knockdown accompanied by lesions of the contralateral amygdala, impede goal-directed response selection, implicating BDNF-expressing oPFC projection neurons in selecting actions based on their consequences. The TrkB agonist 7,8-dihydroxyflavone rescues action selection and increases dendritic spine density on excitatory neurons in the oPFC. Rho-kinase inhibition also rescues goal-

Correspondence: Shannon L. Gourley, Yerkes National Primate Research Center, 954 Gatewood Rd. NE, Atlanta GA 30329, 404-727-2482; fax 404-727-8070, shannon.l.gourley@emory.edu.

All authors report no biomedical financial interests or potential conflicts of interest.

directed response strategies, linking neural remodeling with outcome-based decision-making. Finally, DREADD-mediated oPFC inhibition weakens new action-outcome conditioning.

Conclusions—Activity- and BDNF-dependent neuroplasticity within the oPFC coordinate outcome-based decision-making through interactions with the amygdala. These interactions brake reward-seeking habits, a putative factor in multiple psychopathologies.

Keywords

orbital; habit; amygdala; action; outcome; striatum

Introduction

The orbitofrontal cortex (oPFC) is essential for encoding information about rewards and translating this information into behavioral response strategies. Accordingly, both rodents and non-human primates with lesions or inactivation of the oPFC fail to modify reward-seeking behaviors when a reinforcer loses value (*e.g.*,(1),(2)). Further, the oPFC is essential to value judgment (3) and outcome expectancy (4). In other words, across species, the oPFC is critical for acquiring information relevant to salient outcomes.

These findings raise the possibility that the oPFC may guide decision-making strategies based not just on outcome *value* or reward-related cues, but also on other outcome-related information such as the *likelihood* that a given response will result in a desired outcome. In line with this perspective, recent reports indicate that oPFC-striatal interactions are preferentially engaged during goal-directed, as opposed to habitual, decision-making (5). Further, perturbations in oPFC-striatal interactions – through lesions, inactivation, hyper-activation, or targeted neurotrophin knockdown – result in involuntary motor movements, as well as inflexible habits (5–7).

In addition to the striatum, the oPFC innervates the basolateral nucleus of the amygdala (BLA) (8), which is also necessary for goal-directed decision-making – that is, selecting an action based on the value of an anticipated reinforcer, or based on the likelihood that it will be reinforced (9). From a circuit-level perspective, most reports in this domain have focused on BLA interactions with the nucleus accumbens and dorsal striatum (10–12), meaning top-down cortical regulation of BLA-dependent goal-directed decision-making is under-characterized. Further, these and related studies have largely used lesion approaches in rats, leaving molecular mechanisms unclear. Finally, most studies of the BLA utilize outcome devaluation procedures, which assess decision-making based on the *value* of a goal, rather than the predictive relationship between a response and a reinforcer.

In the present studies, we first report that mouse oPFC-amygdala and oPFC-striatal projection patterns are homologous to those of rats (8,13). Then, we use *in vivo* viral-mediated gene transfer in mice to inactivate the neuroplasticity-associated neurotrophin *Brain-derived neurotrophic factor* (*Bdnf*), or Designer Receptors Exclusively Activated by Designer Drugs (DREADDs) to dampen neural activity, and test a model in which plasticity in the ventrolateral oPFC (VLO) coordinates goal-directed action selection. We also used asymmetric infusion techniques to establish the functional necessity of VLO-BLA

connectivity in selecting actions based on their consequences. We then attempted to augment goal-directed action selection using the TrkB agonist 7,8-dihydroxyflavone (7,8-DHF). Based on our evidence that 7,8-DHF induces dendritic spine proliferation, we last capitalized on the availability of a blood brain barrier-penetrant Rho-kinase inhibitor to rescue outcome-based decision-making following *Bdnf* knockdown. Together, our findings indicate that VLO *Bdnf* systems critically organize goal-directed decision-making via interaction with the downstream BLA.

Methods

For additional details, see Supplementary Materials.

Subjects

Mice were males, >8 weeks old. For studies involving *Bdnf* knockdown, mice were homozygous for a floxed allele (exon V) encoding the *Bdnf* gene (14). These mice were maintained on a mixed BALB/C background. For studies involving dendritic spine imaging, mice expressed *thy1*-derived YFP (15) and were fully back-crossed onto a C57BL/6 background. Other experiments used wildtype C57BL/6 mice, and all original breeding pairs were purchased from Jackson Labs. Throughout, littermates were represented in both control and experimental groups.

Mice were maintained on a 12-hour light cycle (0700 on) and provided food and water *ad libitum* except during instrumental conditioning, when body weights were maintained at ~93% of baseline to motivate responding. Procedures were approved by the Emory University IACUC.

Intracranial infusions

Using standard stereotaxic procedures and coordinates based on (16), the following were delivered: biotinylated dextran amine (BDA)-10,000 (0.15μl/site); lentiviral vectors expressing Cre-Recombinase or GFP under the CMV promoter (0.5μl/site) (Emory Viral Vector Core); or adeno-associated viruses (AAV5)-CaMKII-HA-hM$_4$D(Gi)-IRES-mCitrine or AAV5-CaMKII-GFP (0.5μl/site) (UNC Viral Vector Core). For disconnection experiments, VLO infusions were unilateral, and NMDA (20μg/μl) or saline (0.1μl/site) was infused in the ipsilateral or contralateral BLA.

Instrumental conditioning

Mice were trained to nose poke for food reinforcement (20mg pellets; Bioserv) using Med-Associates conditioning chambers. Training was initiated with a fixed ratio 1 schedule of reinforcement; 30 pellets were available for responding on each of 2 distinct nose poke recesses located on opposite sides of a single wall within the chambers, resulting in 60 pellets/session. Sessions ended when all 60 pellets were delivered or at 135min. Unless otherwise indicated, after 5 sessions, mice were shifted to a random interval (RI) 30-second schedule of reinforcement for 2 sessions; again, 30 pellets were available for responding on each of 2 apertures. At this point, sensitivity to instrumental contingency degradation was tested, or in the case of extended training, mice were trained for an additional 6 RI30-second

sessions and then 7 RI60-second sessions to promote the formation of stimulus-response habits (17). Response acquisition curves represent total responses/min.

A modified version of classical instrumental contingency degradation was used. As previously described (*e.g.*,18,19), in the "non-degraded session", one nose poke aperture was occluded, and responding on the other aperture was reinforced using a variable ratio 2 schedule of reinforcement for 25min. In the "degraded session", the opposite aperture was occluded, and reinforcers were delivered into the magazine for 25min. at a rate matched to each animal's reinforcement rate the previous day. Responding produced no programmed consequences. Thus, one response became significantly more predictive of reinforcement than the other (see(20)). Both apertures were available during a subsequent 10min. probe test, conducted in extinction. In the "disconnection" experiment, this 3-day process was repeated.

Extinction conditioning

After testing as above, mice in one experiment were placed in the conditioning chambers for an additional 15min./day for 7 days. Responding was not reinforced, and mice were injected with vehicle or 7,8-DHF immediately after each session. A subset of these mice was *thy1*-YFP-expressing, to allow for dendritic spine imaging described below. YFP- and non-YFP-expressing mice did not differ in response extinction.

Drugs

7,8-DHF (Sigma; 5mg/kg, 17% DMSO), fasudil (LC Laboratories; 10mg/kg, PBS), ANA-12 (Sigma; 0.5mg/kg, 1% DMSO), CNO (Sigma; 1mg/kg, 2% DMSO), or the corresponding vehicle was administered *i.p.* immediately following action-outcome contingency degradation (7,8-DHF, CNO), immediately prior to contingency degradation (ANA-12), or immediately following extinction training (7,8-DHF). Groups were assigned by matching mice based on response rates during training.

Dendritic spine imaging and enumeration

Dendritic spine imaging was accomplished as described (18,21). 40μm-thick sections were generated from YFP-expressing brains, and unobstructed dendritic segments running parallel to the surface of the section were imaged using a 0.1μm step size. Collapsed z-stacks were analyzed using ImageJ: Each protrusion <4μm was considered a spine and counted (22). Each animal contributed a single density value (its average) to statistical analyses. A single blinded rater scored all spines.

Histology

Brains were sectioned into 55μm-thick sections. BDA signal was amplified with a Vectastain Elite ABC kit and revealed by nickel-enhanced-diaminobenzidine staining. Maximum diffusion around the infusion site was mapped, and patterns of axon terminals downstream of each infusion site were transposed onto representative coronal sections from (16). Labeling from 2–3 mice was analyzed/site.

Following viral vector delivery, every third section was imaged for GFP or mCitrine, or immunostained for Cre (Sigma; 1:750) as appropriate.

To confirm lesion sites, every third section was immunostained for Glial Fibrillary Acidic Protein (GFAP) (Dakocytomation; 1:1000) as described (23).

BDNF quantification

Mice were rapidly decapitated, and brains were frozen on dry ice for BDNF quantification by enzyme-linked immunosorbent assay (ELISA). The VLO and amygdala were extracted with 1mm bilateral tissue punches. ELISA was performed in accordance with manufacturer's instructions (Promega) except the extraction step was excluded. BDNF concentrations were normalized to the total protein content in each sample. Concentrations were normalized to the mean of the control samples on the same plate to control for fluorescence variance across plates.

Statistical analyses

Two-tailed statistical analyses with $\alpha<0.05$ were performed using SigmaStat or SPSS. Tukey's post-hoc t-tests were utilized in the event of interaction effects; posthoc comparisons are indicated graphically. Values lying >2 standard deviations outside of the mean were considered outliers and excluded (see Supplementary Materials). BDNF covariance with behavioral measures was tested using a linear regression analysis.

Results

The mouse oPFC innervates the dorsal striatum and amygdala

We first compared projection patterns between the well-studied dorsolateral oPFC/agranular insula (DLO/AI) and the adjacent VLO. BDA infusion into the VLO (fig. 1a) revealed innervation of both the dorsal striatum and amygdala to be overwhelmingly ipsilateral. The central aspect of the dorsal striatum received heavy innervation broadly along the rostrocaudal axis (fig. 1b). By contrast, only light labeling was present in the ventral striatum. Fibers entered the rostral striatum through the genu of the corpus callosum (gcc) and the external capsule, then formed multiple fiber bundles that coursed through the dorsomedial terminal fields along the rostrocaudal axis.

Within the amygdala, VLO-originating fibers largely spared the lateral amygdala and instead targeted the BLA (fig. 1c–d). In rostral sections, innervation was widely distributed, but in more caudal sections, labeling became laterally oriented along the external capsule. Light innervation of the medial intercalated masses was noted, but the central nucleus was relatively devoid of labeled terminals.

The DLO/AI (fig. 2a) also innervated the central aspects of the dorsal striatum. Unlike the VLO, the DLO/AI also targeted aspects of the lateral and ventral striatum (fig. 2b). Fibers originating from the DLO/AI reached the rostral striatum through the gcc and the external capsule and were organized into fiber bundles. Projections from the DLO/AI to the amygdala were again topographically organized; the heaviest labeling was identified in the rostral BLA, and terminals were densest along the lateral wall (fig. 2c–d). As reported (8),

mid-amygdaloid labeling was primarily evident in the lateral basal nucleus, along with the ventral lateral amygdala. The majority of posterior terminals were located in the ventrolateral field of the basal nucleus (fig. 2c–d).

Projections from the DLO/AI to the amygdala appeared ipsilateral; however, unlike the VLO, innervation of the striatum was evident in both hemispheres, strongest ipsilateral to the infusion site (fig. 3a), culminating in a massive innervation of the posterior caudate (fig. 3b). Additionally of note was the presence of terminals and fibers of passage in the perirhinal cortex (PRh) originating from the DLO/AI, suggesting a DLO/AI-perirhinal-hippocampus pathway in mice similar to that found in macaques (24,25) (fig. 3c).

Overall, VLO *vs.* DLO/AI innervation patterns resembled those in rats (8,26,27), as well as other reports in mice (5,28–30).

VLO BDNF coordinates outcome-based decision-making

The mouse VLO innervates the dorsal striatum and BLA, regions associated with goal-directed action selection (9,31). The VLO might thus *itself* regulate decision-making based on the predictive relationship between an action and an outcome. To test this, we used a task in which mice are trained to generate two food-reinforced responses, then the likelihood that one response will be reinforced is reduced (action-outcome contingency degradation). Meanwhile, the other response remains reinforced in a separate training session (fig. 4a). During a subsequent probe test, mice can generate both responses freely; preferential engagement of the response that is likely to be reinforced is considered “goal-directed,” while non-selective responding is considered habit-based. Throughout these experiments, response acquisition curves reflect both responses; mice did not generate response biases that would interfere with subsequent experimental stages.

The neuroplasticity-associated neurotrophin *Bdnf* was knocked down in the VLO using viral vector strategies, reducing regional BDNF expression [Mann-Whitney U=17, p=0.04](fig. 4b–c). During response training, response rates in the knockdown group lagged, particularly in later sessions when the reinforcement schedule escalated from a fixed ratio to RI [interaction $F_{(6,66)}$=3.8, p=0.006](fig. 4c). This profile is associated with impaired action-outcome decision-making (32). Indeed, *Bdnf* knockdown mice subsequently failed to differentiate between responses that were more, or less, likely to be reinforced, instead relying on habit-based strategies, generating both responses equivalently [interaction $F_{(1,22)}$=9, p=0.007](fig. 4d).

Cortical pyramidal neurons provide BDNF to downstream substrates (33,34). Accordingly, BDNF in the amygdala was reduced following knockdown in the VLO [t_{27}=3, p=0.005](fig. 4e). Further, amygdala BDNF levels correlated with response strategies — higher levels of BDNF were associated with avoidance of the response that was unlikely to be reinforced (r=0.53, p=0.05), while “low” BDNF was associated with habits (fig. 4e).

BDNF-expressing amygdala-targeted VLO projection neurons may thus regulate goal-directed action selection. To test this model, we modified classical disconnection procedures in which contralateral lesions would be placed unilaterally in the VLO and BLA, instead

knocking down *Bdnf* unilaterally in the VLO and placing a lesion in the contralateral amygdala (fig. 5a). All mice acquired the instrumental responses, with no differences between groups (F<1)(fig. 5b). Thus, the response acquisition deficits following bilateral *Bdnf* knockdown (fig. 4c) cannot obviously be attributed to effects on VLO-BLA interactions. Nonetheless, contralateral infusions resulted in habitual response patterns [interaction $F_{(2,30)}$=4.9, p<0.05](fig. 5c). By contrast, ipsilateral infusions, leaving one cortico-amygdala circuit intact, spared response selection.

With additional contingency degradation training, mice with contralateral infusions ultimately differentiated between the responses [effect of choice p<0.05](fig. 5c). Thus, interfering with BDNF-dependent VLO-amygdala interactions delays, but *does not fully block*, goal-directed response selection.

TrkB regulates goal-directed decision-making

Next, we assessed the role of the high-affinity BDNF receptor TrkB using the small-molecule agonist 7,8-DHF (35). Intact mice were extensively trained such that they would develop stimulus-response habits by virtue of over-training. Response rates did not differ between mice designated to vehicle or 7,8-DHF groups (Fs<1)(fig. 6a). We then violated the predictive relationship between one response and the associated reinforcer and injected mice immediately following this training session, during the presumptive consolidation of new learning. Vehicle-treated mice failed to differentiate between the responses that were more, or less, likely to be reinforced the following day, relying instead on familiar habit-based strategies. By contrast, 7,8-DHF caused a 2-fold preference for the response likely to be reinforced [interaction $F_{(1,12)}$=6.2, p=0.03](fig. 6b).

We replicated this experiment, additionally pretreating mice with the TrkB antagonist ANA-12 (36). Groups did not differ during training (Suppl. fig. S1). ANA-12 blocked 7,8-DHF [interaction $F_{(1,29)}$=8, p=0.009](fig. 6c), evidence that 7,8-DHF enhances the consolidation of action-outcome conditioning in a TrkB-dependent manner. Unexpectedly, mice that received both ANA-12 and 7,8-DHF preferentially engaged the response that was unlikely to be reinforced, though this effect may be driven by relatively few mice (fig. 6c, right).

Separate mice were trained to nose poke using a fixed ratio 1 schedule of reinforcement (fig. 6d) to confirm that systemic 7,8-DHF had no effects at a time point when typical mice would be expected to be “goal-directed” [main effect $F_{(1,13)}$=71.2, p<0.001](fig. 6e). This is important because prelimbic PFC-targeted BDNF microinfusions, under certain circumstances, cause habit-like behavior (18,37).

Sensitivity to action-outcome contingency degradation and nonreinforcement (extinction) are dissociable (38), and the oPFC does not appear to be a site of extinction consolidation in appetitive contexts (39). On the other hand, 7,8-DHF *enhances* the extinction of conditioned freezing (40), suggesting that it may also regulate the extinction of an appetitive response. We trained mice further until responding was robust (>4 responses/min), then withheld reinforcement. Despite injections following several training sessions, 7,8-DHF did not impact response extinction (Fs<1)(fig. 6f). Following response extinction, we enumerated

dendritic spines in the VLO and found that 7,8-DHF increased dendritic spine density on excitatory neurons in layer V (fig. 6g).

Correction of response strategies following VLO *Bdnf* silencing

Stimulating TrkB enhances the ability of mice to select actions based on their consequences. We thus next assessed whether 7,8-DHF could recover response strategies in *Bdnf* knockdown mice. We additionally treated a group with the Rho-kinase inhibitor fasudil, motivated by evidence that TrkB stimulation suppresses p75-mediated signaling, which can otherwise inhibit neurite outgrowth via substrates such as Rho-kinase (41). Again, injections were administered immediately following action-outcome contingency degradation training, and response rates represent responding, drug-free, during a subsequent probe test.

Response rates did not differ during training [“to be 7,8-DHF” *vs.* “to be saline” *vs.* “to be fasudil” Fs<1](fig. 6h). As expected, *Bdnf* knockdown reduced rates (main effect of *Bdnf,* p=0.04). Subsequently, vehicle-treated mice with VLO-targeted *Bdnf* knockdown failed to differentiate between the responses that were more, or less, likely to be reinforced. By contrast, knockdown mice treated with 7,8-DHF or fasudil preferentially engaged the response likely to be reinforced in a goal-directed fashion [*Bdnf* × 7,8-DHF $F_{(1,37)}$=4, p=0.05; fasudil t_5=2.6, p=0.047](fig. 6i). During this probe test, control mice generated >60% of responses toward the intact action-outcome contingency; this preference dropped to chance levels in knockdown mice. Response preference was fully rescued by 7,8-DHF and fasudil [$F_{(4,39)}$=6.8, p<0.001; all groups compared to Cre-only, p<0.04](fig. 6j).

Additionally, fasudil did not impact response choice in typical mice with the same training history (Suppl. fig. S2).

Gi-DREADD stimulation impairs goal-directed action selection

Last, a CaMKII-Gi-DREADD or GFP was expressed in the VLO (fig. 7a), allowing us to acutely manipulate neuroplasticity in glutamatergic VLO projection neurons. Response rates did not differ between groups during training (Fs<1)(fig. 7b). The synthetic ligand CNO was then administered systemically to all mice following instrumental contingency degradation training. GFP-expressing mice subsequently preferentially generated the response most likely to be reinforced [main effect $F_{(1,6)}$=7.1, p=0.04](fig. 7c, left), while Gi-DREADD-expressing mice initially engaged the response most likely to be reinforced, but this effect decayed, and responding became non-selective [interaction $F_{(1,5)}$=24.6, p=0.004](fig. 7c, right). An overall interaction further indicated that Gi-DREADD stimulation weakened goal-directed response strategies [$F_{(1,11)}$=5.1, p<0.05](fig. 7d).

Discussion

Considerable evidence indicates that the oPFC encodes salient information regarding desirable outcomes, such as external cues signaling reinforcement, as well as the value of rewards (2). The oPFC may also guide outcome-based decision-making based on other reinforcement-related information such as the likelihood that a given behavior will be reinforced, but to date, relatively few investigations into oPFC function have focused on action-outcome associative learning and memory. We addressed this gap by first verifying

that two important subregions of the oPFC — the VLO and DLO/AI — innervate the amygdala in mice in patterns similar to those reported in rats (8). Next we used a combination of site-selective gene silencing and pharmacological interventions to demonstrate that: *1)* VLO-derived BDNF is required for selecting actions based on their consequences; *2)* obstructing BDNF-dependent functional connectivity between the VLO and amygdala impairs this type of goal-directed decision-making, resulting in habit-like behaviors; *3)* habitual response strategies induced by either extended training or selective VLO *Bdnf* knockdown can be reversed by the TrkB agonist, 7,8-DHF, or the Rho-kinase inhibitor, fasudil; and *4)* DREADD-mediated inhibition of glutamatergic neuroplasticity in the VLO disrupts the consolidation of new information regarding the predictive relationship between actions and their outcomes, weakening goal-directed response strategies.

We have previously reported that knocking down *Bdnf* in the VLO impairs goal-directed response selection (7). Here, we first highlight that the VLO innervates the BLA, an amygdalar subdivision involved in multiple forms of associative conditioning (9,42,43). Although less dense than those originating from the adjacent DLO/AI subregions, these projections are consistent with those reported in monkeys (44,45) and rats (8), as well as other investigations in mice (5,28–30). Conservation across species suggests that these networks are essential for evolutionarily-conserved behaviors, such as learning that specific actions produce desired outcomes, and that the VLO is positioned to provide top-down regulation of these processes. This may occur via local plasticity within the VLO that in turn coordinates differential excitatory outputs. Additionally, the VLO may affect plasticity in the BLA via axonal transport of small peptides such as BDNF. Indeed, BDNF expression *in the amygdala* was diminished following VLO *Bdnf* knockdown, and BDNF protein levels predicted response selection strategies.

VLO-BLA projections are ipsilateral. We capitalized on this segregated neuroanatomy by knocking down VLO *Bdnf* unilaterally and ablating the contralateral amygdala, leaving the infected VLO to project to the one remaining healthy amygdala. This “disconnection” approach allowed us to assess the impact of BDNF-dependent VLO-BLA interactions on response choice. Disconnection caused outcome-insensitive habits, recapitulating the effects of bilateral VLO *Bdnf* knockdown. Goal-directed responding was intact in mice with ipsilateral infusions in which one oPFC-amygdala circuit remained intact, further indicating that BDNF-mediated plasticity between these structures is fundamental to selecting actions based on their consequences.

TrkB regulates the consolidation of action-outcome conditioning

VLO *Bdnf* knockdown impaired goal-directed action selection, raising the possibility that TrkB stimulation could *rescue*, or *enhance*, action-outcome conditioning. We tested this by first inducing habits in mice using a classical approach – response over-training (46) – then stimulated TrkB during the period immediately following action-outcome instrumental contingency degradation, when mice could be presumably consolidating new information regarding the predictive relationships between actions and their outcomes (namely, that one action is no longer likely to be reinforced). The TrkB agonist 7,8-DHF enhanced action-outcome conditioning, resulting in goal-directed action selection in a subsequent probe test.

These and other reports suggest that a latent “goal-directed” system can be accessed even once habits have developed (47), and our findings indicate that this process is TrkB-sensitive.

7,8-DHF also enhanced action-outcome conditioning in mice with VLO-targeted *Bdnf* knockdown, suggesting that BDNF organizes action selection through its high-affinity receptor TrkB, as opposed to pro-BDNF binding to the p75 receptor. Additionally, 7,8-DHF could be blocked by pretreatment with ANA-12, a TrkB antagonist, indicating that the actions of 7,8-DHF can be attributed, at least in part, to TrkB stimulation, rather than off-target effects.

In these experiments, we administered 7,8-DHF immediately following action-outcome contingency degradation, rather than at the probe test when mice must choose between responses that are more, or less, likely to be reinforced. This experimental design was motivated by evidence that temporary inactivation of the BLA during outcome devaluation training occludes goal-directed response selection during a subsequent probe test, while inactivation *during* the probe test has no effects (48–50). Thus, the BLA is essential for learning about, but not necessarily expressing, goal-directed decision-making strategies. Injections immediately following the training sessions additionally allowed us to avoid drug effects on the *acquisition* of instrumental contingency degradation training and instead target the consolidation phase of new learning.

Considerable attention has been given to the functional significance of projections *from* the BLA *to* the oPFC (51,52). While we have instead focused on oPFC projections *to* the BLA, it seems probable that bidirectional interactions regulate BDNF-dependent action selection. For example, 7,8-DHF increased dendritic spine density in deep-layer VLO. This spine population is targeted by BLA projections (53), so it is conceivable that 7,8-DHF corrected decision-making strategies in a *direct* manner by restoring VLO TrkB binding following local *Bdnf* knockdown, and in an *indirect* manner by structurally remodeling these neurons to support greater synaptic connectivity and increased sensitivity to BLA inputs. Supporting this “indirect” model, Rho-kinase inhibition mimicked 7,8-DHF, also correcting decision-making strategies in *Bdnf*-deficient mice. This is significantly because Rho-kinase provides a contractile force on the actin cytoskeleton, the structural lattice that forms the shape of neurons; this can be inhibited by TrkB-mediated interference with p75 signaling, allowing for structural plasticity (41). A final consideration is that 7,8-DHF may additionally regulate action selection strategies by increasing TrkB binding *in the amygdala*, particularly given that 7,8-DHF facilitates long-term potentiation in this region (54).

Based on the association between structural plasticity in the VLO and regulation of action selection strategies, as well as evidence that BDNF release from axons of pyramidal neurons is activity-dependent (55,56), we lastly applied a CaMKII-Gi-coupled DREADD to excitatory VLO neurons. When the synthetic ligand CNO is administered, an inhibitory Gi pathway is acutely activated, reducing the likelihood that Gi-DREADD-expressing neurons will generate activity-dependent action potentials or release glutamate from neuron terminals (57). Impeding activity-dependent excitatory transmission in this manner disrupted consolidation processes associated with developing goal-directed action selection strategies,

rendering the memory of contingency degradation training inherently labile. The effect was, interestingly, weaker than that of *Bdnf* knockdown; whether *Bdnf* knockdown causes both acute and chronic neurobiological sequelae that contribute to habit formation will be a topic of future consideration.

Conclusions

Our findings implicate a BDNF-sensitive VLO-amygdala neurocircuit in the coordination of actions and habits. These findings may provide mechanistic insight into evidence implicating oPFC *Bdnf* in psychopathologies such as addiction. For instance, cocaine seeking in rats has been associated with elevated oPFC *Bdnf* (58), while diminished oPFC *Bdnf* increases sensitivity to cocaine-associated conditioned stimuli (7). Given our current findings, it is tempting to speculate that drug-related oPFC *Bdnf* overexpression drives goal-oriented drug seeking, while the atrophy of oPFC neurotrophin systems – caused by stressor exposure, for example (59) – can drive habitual drug seeking. A second important aspect of this report pertains to the identification of experimental techniques that reverse habits, which has otherwise proven challenging in the field. We find that TrkB- and Rho-kinase-targeted drugs, when administered during the consolidation of new action-outcome associative conditioning, may serve as promising adjuncts to behavioral therapies aimed at suppressing or reversing habitual, maladaptive thought or behavioral patterns.

Supplementary Material

Refer to Web version on PubMed Central for supplementary material.

Acknowledgments

We thank Ms. Amanda Allen and Mr. Zach Liang for their contributions. This work was supported by T32DA015040, P51OD11132, P30NS055077, DA034808, DA036737, Children's Healthcare of Atlanta, the Brain and Behavior Research Foundation when Dr. Gourley was the Foundation's Katherine Deschner Family Investigator, and an NIMH BRAINS award to Dr. Gourley (MH101477). We thank Ms. Lauren Shapiro, and Drs. Geoffrey Schoenbaum and Christopher Muly for guidance and valuable feedback.

References

1. Rhodes SE, Murray EA. Differential effects of amygdala, orbital prefrontal cortex, and prelimbic cortex lesions on goal-directed behavior in rhesus macaques. J Neurosci. 2013; 33:3380–3389. [PubMed: 23426666]
2. McDannald MA, Jones JL, Takahashi YK, Schoenbaum G. Learning theory: a driving force in understanding orbitofrontal function. Neurobiol Learn Mem. 2014; 108:22–27. [PubMed: 23770491]
3. Padoa-Schioppa C. Neurobiology of economic choice: a good-based model. Annu Rev Neurosci. 2011; 34:333–359. [PubMed: 21456961]
4. Schoenbaum G, Roesch MR, Stalnaker TA, Takahashi YK. A new perspective on the role of the orbitofrontal cortex in adaptive behaviour. Nat Rev Neurosci. 2009; 10:885–892. [PubMed: 19904278]
5. Gremel CM, Costa RM. Orbitofrontal and striatal circuits dynamically encode the shift between goal-directed and habitual actions. Nat Commun. 2013; 4:2264. [PubMed: 23921250]
6. Ahmari SE, Spellman T, Douglass NL, Kheirbek MA, Simpson HB, Deisseroth K, et al. Repeated cortico-striatal stimulation generates persistent OCD-like behavior. Science. 2013; 340:1234–1239. [PubMed: 23744948]

7. Gourley SL, Olevska A, Zimmermann KS, Ressler KJ, Dileone RJ, Taylor JR. The orbitofrontal cortex regulates outcome-based decision-making via the lateral striatum. Eur J Neurosci. 2013; 38:2382–2388. [PubMed: 23651226]
8. McDonald AJ, Mascagni F, Guo L. Projections of the medial and lateral prefrontal cortices to the amygdala: a Phaseolus vulgaris leucoagglutinin study in the rat. Neuroscience. 1996; 71:55–75. [PubMed: 8834392]
9. Balleine BW, Killcross AS, Dickinson A. The effect of lesions of the basolateral amygdala on instrumental conditioning. J Neurosci. 2003; 23:666–675. [PubMed: 12533626]
10. Wang SH, Ostlund SB, Nader K, Balleine BW. Consolidation and reconsolidation of incentive learning in the amygdala. J Neurosci. 2005; 25:830–835. [PubMed: 15673662]
11. Shiflett MW, Balleine BW. At the limbic-motor interface: disconnection of basolateral amygdala from nucleus accumbens core and shell reveals dissociable components of incentive motivation. Eur J Neurosci. 2010; 32:1735–1743. [PubMed: 21044174]
12. Corbit LH, Leung BK, Balleine BW. The role of the amygdala-striatal pathway in the acquisition and performance of goal-directed instrumental actions. J Neurosci. 2013; 33:17682–17690. [PubMed: 24198361]
13. Mailly P, Aliane V, Groenewegen HJ, Haber SN, Deniau JM. The rat prefrontostriatal system analyzed in 3D: evidence for multiple interacting functional units. J Neurosci. 2013; 33:5718–5727. [PubMed: 23536085]
14. Rios M, Fan G, Fekete C, Kelly J, Bates B, Kuehn R, et al. Conditional deletion of brain-derived neurotrophic factor in the postnatal brain leads to obesity and hyperactivity. Mol Endocrinol. 2001; 15:1748–1757. [PubMed: 11579207]
15. Feng G, Mellor RH, Bernstein M, Keller-Peck C, Nguyen QT, Wallace M, et al. Imaging neuronal subsets in transgenic mice expressing multiple spectral variants of GFP. Neuron. 2000; 28:41–51. [PubMed: 11086982]
16. Paxinos, G.; Franklin, KBJ. The Mouse Brain in Stereotaxic Coordinates. second. San Diego: Academic Press; 2001.
17. Dickinson A, Nicholas D, Adams CD. The effect of the instrumental training contingency on susceptibility to reinforcer devaluation. The Quarterly Journal of Experimental Psychology. 1983; 35:35–51.
18. Gourley SL, Swanson AM, Jacobs AM, Howell JL, Mo M, Dileone RJ, et al. Action control is mediated by prefrontal BDNF and glucocorticoid receptor binding. Proc Natl Acad Sci U S A. 2012; 109:20714–20719. [PubMed: 23185000]
19. Swanson AM, Shapiro LP, Whyte AJ, Gourley SL. Glucocorticoid receptor regulation of action selection and prefrontal cortical dendritic spines. Commun Integr Biol. 2013; 6:e26068. [PubMed: 24563705]
20. Hinton EA, Wheeler MG, Gourley SL. Early-life cocaine interferes with BDNF-mediated behavioral plasticity. Learn Mem. 2014; 21:253–257. [PubMed: 24737916]
21. Gourley SL, Swanson AM, Koleske AJ. Corticosteroid-induced neural remodeling predicts behavioral vulnerability and resilience. J Neurosci. 2013; 33:3107–3112. [PubMed: 23407965]
22. Peters A, Kaiserman-Abramof IR. The small pyramidal neuron of the rat cerebral cortex. The perikaryon, dendrites and spines. Am J Anat. 1970; 127:321–355. [PubMed: 4985058]
23. Gourley SL, Lee AS, Howell JL, Pittenger C, Taylor JR. Dissociable regulation of instrumental action within mouse prefrontal cortex. Eur J Neurosci. 2010; 32:1726–1734. [PubMed: 21044173]
24. Suzuki WA, Amaral DG. Cortical inputs to the CA1 field of the monkey hippocampus originate from the perirhinal and parahippocampal cortex but not from area TE. Neurosci Lett. 1990; 115:43–48. [PubMed: 1699176]
25. Van Hoesen G, Pandya DN, Butters N. Some connections of the entorhinal (area 28) and perirhinal (area 35) cortices of the rhesus monkey. II. Frontal lobe afferents. Brain Res. 1975; 95:25–38. [PubMed: 1156867]
26. Schilman EA, Uylings HB, Galis-de Graaf Y, Joel D, Groenewegen HJ. The orbital cortex in rats topographically projects to central parts of the caudate-putamen complex. Neurosci Lett. 2008; 432:40–45. [PubMed: 18248891]

27. Berendse HW, Galis-de Graaf Y, Groenewegen HJ. Topographical organization and relationship with ventral striatal compartments of prefrontal corticostriatal projections in the rat. J Comp Neurol. 1992; 316:314–347. [PubMed: 1577988]
28. Oh SW, Harris JA, Ng L, Winslow B, Cain N, Mihalas S, et al. A mesoscale connectome of the mouse brain. Nature. 2014; 508:207–214. [PubMed: 24695228]
29. Matyas F, Lee J, Shin HS, Acsady L. The fear circuit of the mouse forebrain: connections between the mediodorsal thalamus, frontal cortices and basolateral amygdala. Eur J Neurosci. 2014; 39:1810–1823. [PubMed: 24819022]
30. Dong, H., et al. Mouse Connectome Project. @ http://www.mouseconnectome.org/
31. Yin HH, Ostlund SB, Balleine BW. Reward-guided learning beyond dopamine in the nucleus accumbens: the integrative functions of cortico-basal ganglia networks. Eur J Neurosci. 2008; 28:1437–1448. [PubMed: 18793321]
32. Corbit LH, Balleine BW. The role of prelimbic cortex in instrumental conditioning. Behav Brain Res. 2003; 146:145–157. [PubMed: 14643467]
33. Altar CA, Cai N, Bliven T, Juhasz M, Conner JM, Acheson AL, et al. Anterograde transport of brain-derived neurotrophic factor and its role in the brain. Nature. 1997; 389:856–860. [PubMed: 9349818]
34. Conner JM, Lauterborn JC, Yan Q, Gall CM, Varon S. Distribution of brain-derived neurotrophic factor (BDNF) protein and mRNA in the normal adult rat CNS: evidence for anterograde axonal transport. J Neurosci. 1997; 17:2295–2313. [PubMed: 9065491]
35. Jang SW, Liu X, Yepes M, Shepherd KR, Miller GW, Liu Y, et al. A selective TrkB agonist with potent neurotrophic activities by 7,8-dihydroxyflavone. Proc Natl Acad Sci U S A. 2010; 107:2687–2692. [PubMed: 20133810]
36. Cazorla M, Premont J, Mann A, Girard N, Kellendonk C, Rognan D. Identification of a low-molecular weight TrkB antagonist with anxiolytic and antidepressant activity in mice. J Clin Invest. 2011; 121:1846–1857. [PubMed: 21505263]
37. Graybeal C, Feyder M, Schulman E, Saksida LM, Bussey TJ, Brigman JL, et al. Paradoxical reversal learning enhancement by stress or prefrontal cortical damage: rescue with BDNF. Nat Neurosci. 2011; 14:1507–1509. [PubMed: 22057192]
38. Hammond LJ. The effect of contingency upon the appetitive conditioning of free-operant behavior. J Exp Anal Behav. 1980; 34:297–304. [PubMed: 16812191]
39. Panayi MC, Killcross S. Orbitofrontal cortex inactivation impairs between-but not within-session Pavlovian extinction: an associative analysis. Neurobiol Learn Mem. 2014; 108:78–87. [PubMed: 23954805]
40. Andero R, Heldt SA, Ye K, Liu X, Armario A, Ressler KJ. Effect of 7,8-dihydroxyflavone, a small-molecule TrkB agonist, on emotional learning. Am J Psychiatry. 2011; 168:163–172. [PubMed: 21123312]
41. Reichardt LF. Neurotrophin-regulated signalling pathways. Philos Trans R Soc Lond B Biol Sci. 2006; 361:1545–1564. [PubMed: 16939974]
42. Davis M. The role of the amygdala in fear and anxiety. Annu Rev Neurosci. 1992; 15:353–375. [PubMed: 1575447]
43. Fanselow MS, LeDoux JE. Why we think plasticity underlying Pavlovian fear conditioning occurs in the basolateral amygdala. Neuron. 1999; 23:229–232. [PubMed: 10399930]
44. Groenewegen HJ, Uylings HB. The prefrontal cortex and the integration of sensory, limbic and autonomic information. Prog Brain Res. 2000; 126:3–28. [PubMed: 11105636]
45. Barbas H. Connections underlying the synthesis of cognition, memory, and emotion in primate prefrontal cortices. Brain Res Bull. 2000; 52:319–330. [PubMed: 10922509]
46. Balleine BW, O'Doherty JP. Human and rodent homologies in action control: corticostriatal determinants of goal-directed and habitual action. Neuropsychopharmacology. 2010; 35:48–69. [PubMed: 19776734]
47. Gourley SL, Olevska A, Gordon J, Taylor JR. Cytoskeletal determinants of stimulus-response habits. J Neurosci. 2013; 33:11811–11816. [PubMed: 23864670]
48. Wellman LL, Gale K, Malkova L. GABAA-mediated inhibition of basolateral amygdala blocks reward devaluation in macaques. J Neurosci. 2005; 25:4577–4586. [PubMed: 15872105]

49. West EA, Forcelli PA, Murnen AT, McCue DL, Gale K, Malkova L. Transient inactivation of basolateral amygdala during selective satiation disrupts reinforcer devaluation in rats. Behav Neurosci. 2012; 126:563–574. [PubMed: 22845705]
50. Parkes SL, Balleine BW. Incentive memory: evidence the basolateral amygdala encodes and the insular cortex retrieves outcome values to guide choice between goal-directed actions. J Neurosci. 2013; 33:8753–8763. [PubMed: 23678118]
51. Holland PC, Gallagher M. Amygdala-frontal interactions and reward expectancy. Curr Opin Neurobiol. 2004; 14:148–155. [PubMed: 15082318]
52. Schoenbaum G, Setlow B, Saddoris MP, Gallagher M. Encoding predicted outcome and acquired value in orbitofrontal cortex during cue sampling depends upon input from basolateral amygdala. Neuron. 2003; 39:855–867. [PubMed: 12948451]
53. Ghashghaei HT, Barbas H. Pathways for emotion: interactions of prefrontal and anterior temporal pathways in the amygdala of the rhesus monkey. Neuroscience. 2002; 115:1261–1279. [PubMed: 12453496]
54. Li C, Dabrowska J, Hazra R, Rainnie DG. Synergistic activation of dopamine D1 and TrkB receptors mediate gain control of synaptic plasticity in the basolateral amygdala. PLoS ONE. 2011; 6:e26065. [PubMed: 22022509]
55. Balkowiec A, Katz DM. Cellular mechanisms regulating activity-dependent release of native brain-derived neurotrophic factor from hippocampal neurons. J Neurosci. 2002; 22:10399–10407. [PubMed: 12451139]
56. Gartner A, Staiger V. Neurotrophin secretion from hippocampal neurons evoked by long-term-potentiation-inducing electrical stimulation patterns. Proc Natl Acad Sci U S A. 2002; 99:6386–6391. [PubMed: 11983920]
57. Dong S, Allen JA, Farrell M, Roth BL. A chemical-genetic approach for precise spatio-temporal control of cellular signaling. Mol Biosyst. 2010; 6:1376–1380. [PubMed: 20532295]
58. Hearing MC, Miller SW, See RE, McGinty JF. Relapse to cocaine seeking increases activity-regulated gene expression differentially in the prefrontal cortex of abstinent rats. Psychopharmacology (Berl). 2008; 198:77–91. [PubMed: 18311559]
59. Gourley SL, Kedves AT, Olausson P, Taylor JR. A history of corticosterone exposure regulates fear extinction and cortical NR2B, GluR2/3, and BDNF. Neuropsychopharmacology. 2009; 34:707–716. [PubMed: 18719621]
60. Rosen, G., et al. The mouse brain library. 2000. @ http://www.Mbl.Org. International Mouse Genome Conference

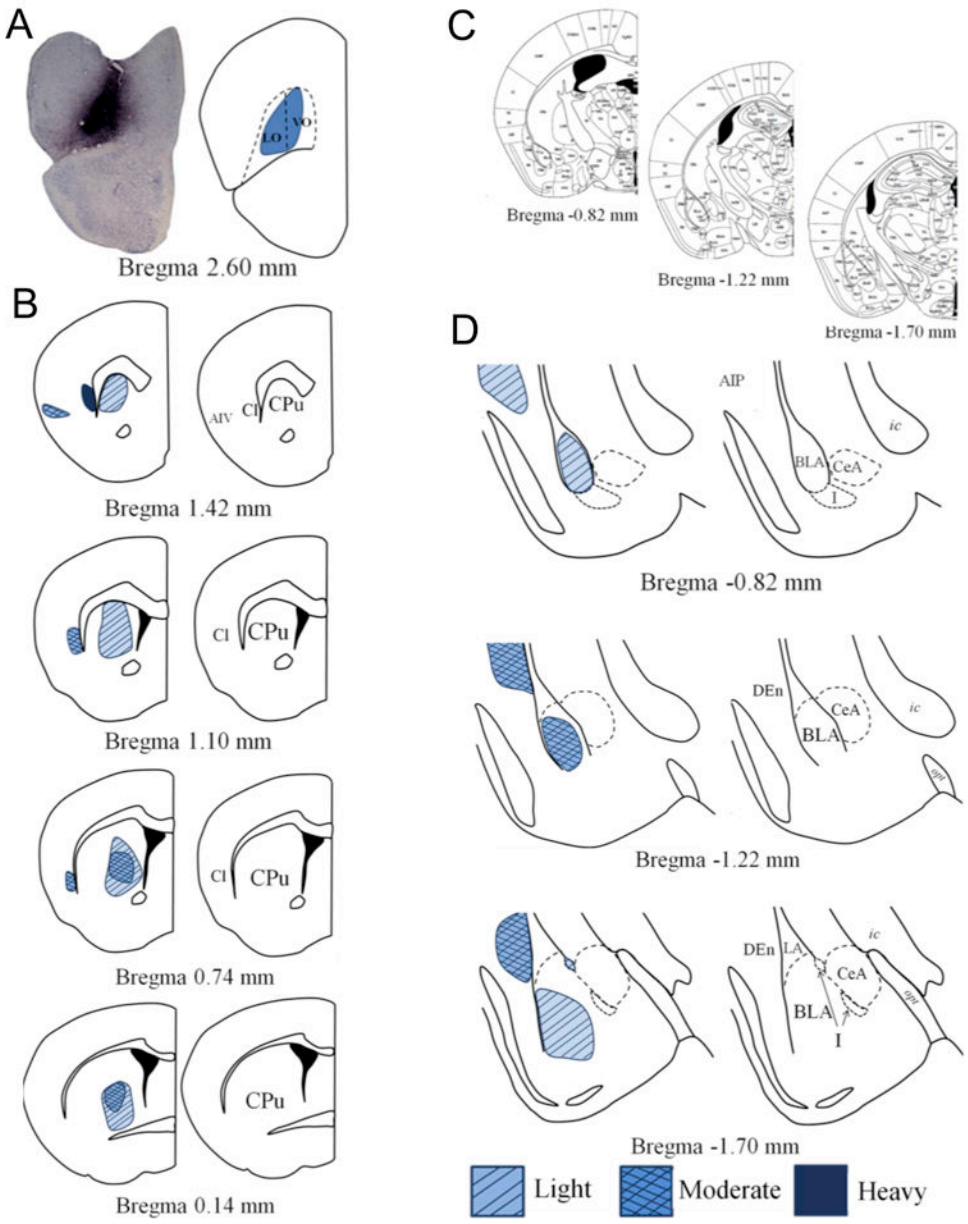

Fig. 1. The VLO innervates the dorsal striatum and BLA

(a) A representative BDA infusion into the VLO and a drawing of the targeted area are shown (distance from bregma and estimated regional boundaries based on (16)). (b) The VLO innervates the dorsomedial and central striatum along the rostrocaudal axis. (c) Coronal amygdala sections from (16) correspond to magnified depictions shown in (d). (d) Infusions of BDA into the VLO reveal innervation of the anterior BLA and the lateral wall of the posterior BLA, along with light innervation of the intercalated cell masses and moderate innervation of the dorsal endopiriform nucleus. Abbreviations: *AIP-posterior agranular insular cortex; AIV-ventral agranular insular cortex; BLA-basolateral amygdala; Cl-claustrum; CPu-caudate putamen; CeA-central amygdala; DEn-dorsal endopiriform nucleus; I-intercalated masses; ic-internal capsule; opt-optic tract.*

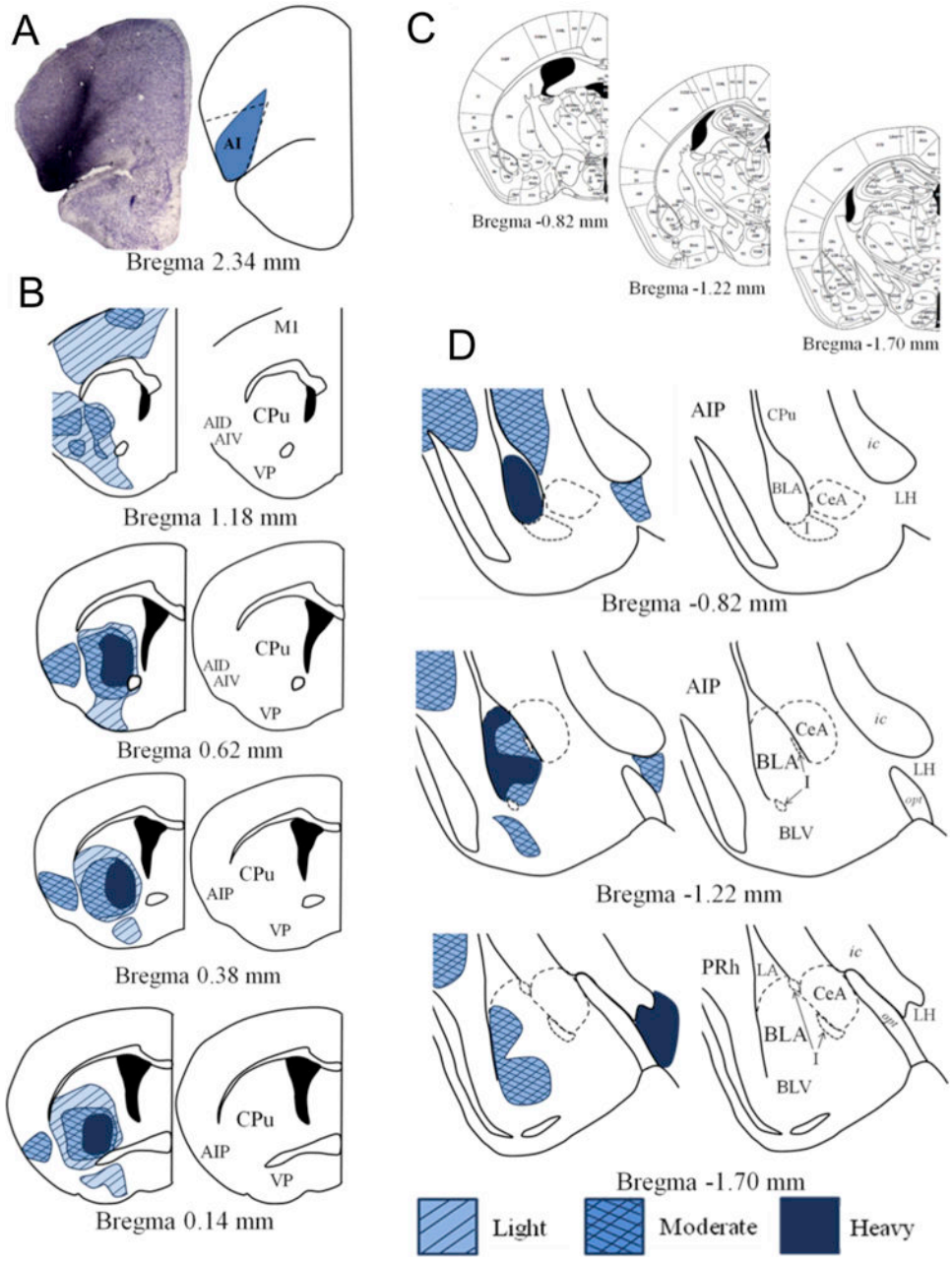

Fig. 2. The DLO/AI innervates the lateral and ventral striatum and BLA

(a) A representative infusion of BDA into the DLO/AI and a rendering of the targeted area are shown. (b) BDA infusions into the DLO/AI illuminate heavy innervation of the ventral and lateral striatum, and reveal innervation of the posterior AI that is maintained along the rostrocaudal axis. (c) Coronal amygdala sections from (16) correspond to the magnified depictions shown in (d). (d) The DLO/AI sends heavy projections to the anterior BLA. Projections are lighter in the posterior BLA, and preferentially terminate along the lateral wall. Innervation is also noted in the ventral BLA, as well as the posterior AI and the PRh. Abbreviations not defined in Fig. 1: *AID-dorsal agranular insular cortex; BLV-basolateral*

amygdala, ventral part; LH-lateral hypothalamus; M1-primary motor cortex; PRh-perirhinal cortex; VP-ventral pallidum.

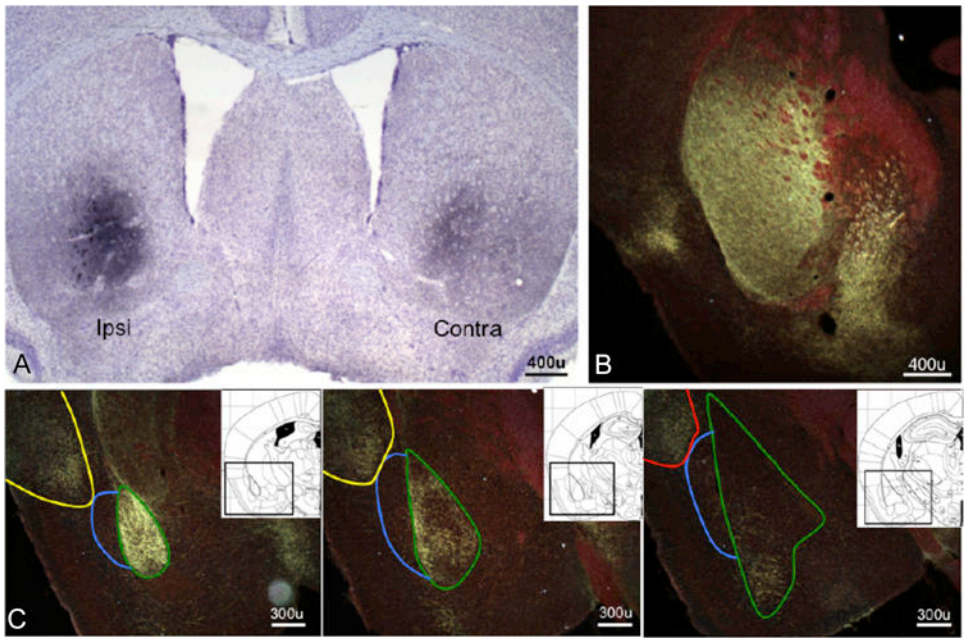

Fig. 3. Photomicrographs show representative BDA staining and demonstrate innervation of the striatum and PRh and BLA by the DLO/AI

(a) Projections from the DLO/AI to the striatum are bihemispheric, but labeling is heaviest in the hemisphere ipsilateral to the infusion site, and (b) heavy labeling is noted in the posterior caudate. (c) Representative images of DLO/AI innervation of the BLA, posterior AI, and PRh (rostral to caudal); note avoidance the dorsal endopiriform nucleus. Green outline-BLA; blue outline-DEn; yellow outline-posterior AI; red outline-PRh. Inset: Corresponding images from (16), with regions outlined in black.

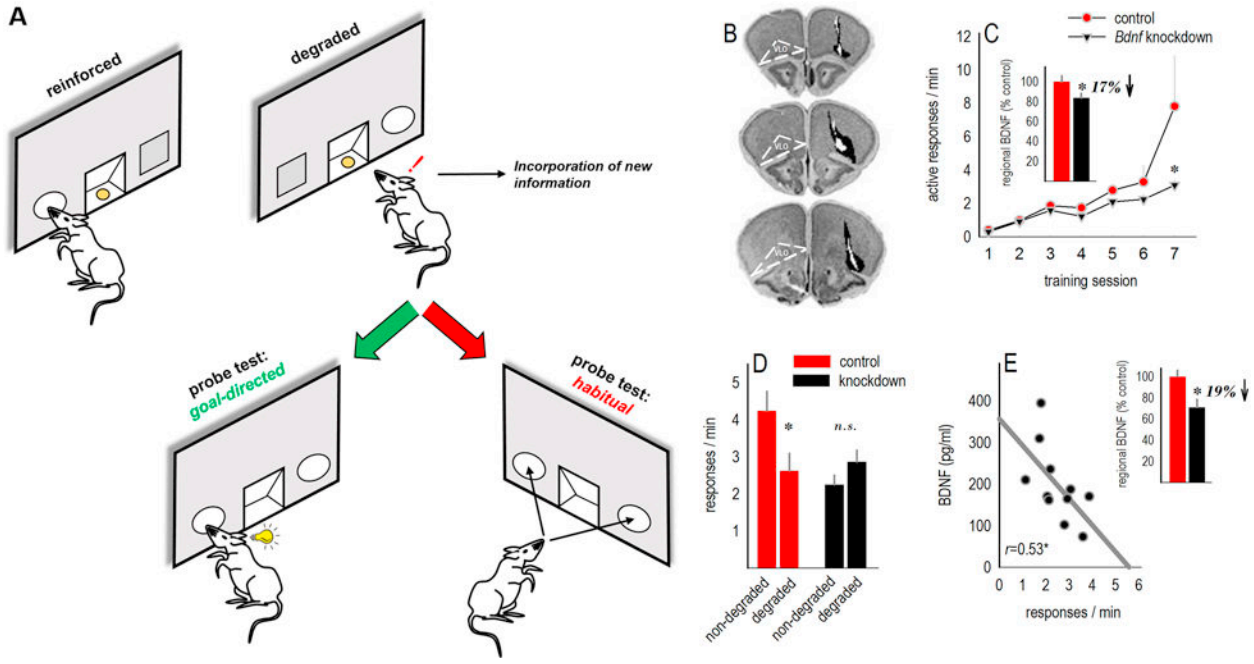

Fig. 4. VLO-selective *Bdnf* knockdown interferes with goal-directed action selection

(a) A task schematic is shown. Mice are trained to generate two distinct responses. Then, the likelihood that one response will be reinforced is decreased. Preferential engagement of the remaining response during a probe test is interpreted as goal-directed action selection, while engaging both responses equivalently — despite contingency degradation — is codified as habitual behavior. (b) *Bdnf* was knocked down bilaterally in the VLO. Infusion sites are summarized on images from (60). Black represents the largest viral vector spread, and white the smallest. (c) Inset: Infusions resulted in decreased BDNF expression in homogenized VLO tissue. Mice were trained to nose poke for food reinforcers; *Bdnf* knockdown reduced response rates, particularly when the response requirement escalated from a fixed ratio 1 to random interval schedule (final 2 sessions). Rates represent total responses on both apertures. (d) Mice with *Bdnf* knockdown were also unable to select between actions that were more, *vs.* less, likely to be reinforced (non-degraded *vs.* degraded) following instrumental contingency degradation; instead, they engaged familiar habit-like response patterns, generating both responses equally. (e) BDNF expression in the downstream amygdala correlated with the degree of impairment following VLO-targeted *Bdnf* knockdown, with low BDNF associated with robust responding on the ‘degraded’ nose poke aperture. Amygdala BDNF expression was also reduced overall in mice with VLO-targeted *Bdnf* knockdown (inset). Symbols and bars represent means+SEMs, except in (e) where each symbol represents a single mouse.*p<0.05.

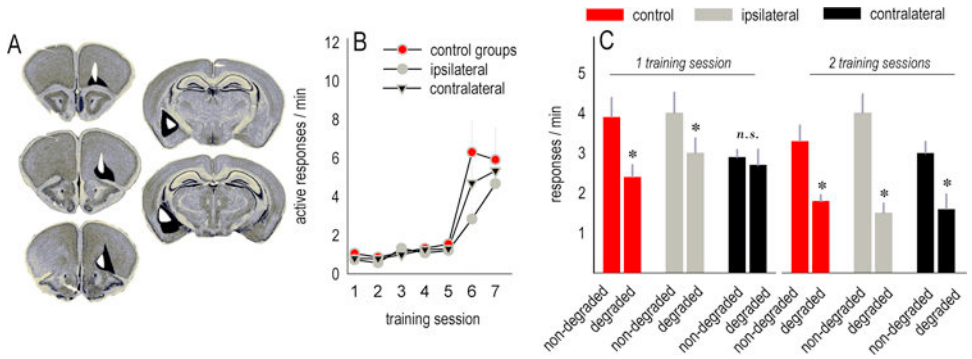

Fig. 5. Functional disconnection of the VLO and amygdala results in habits

(a) Histological representations of unilateral cortical viral vector infusions and amygdala lesions are transposed onto images from (60). Black represents the largest and white the smallest. (b) Mice were trained to nose poke for food reinforcers; response rates did not differ between groups. (c) Mice with asymmetric infusions were, however, insensitive to instrumental contingency degradation. With an additional training session, mice ultimately were able to develop outcome-directed response strategies, indicating that contralateral infusions delayed, but did not block, action-outcome conditioning. Symbols and bars represent means+SEMs,*p<0.05.

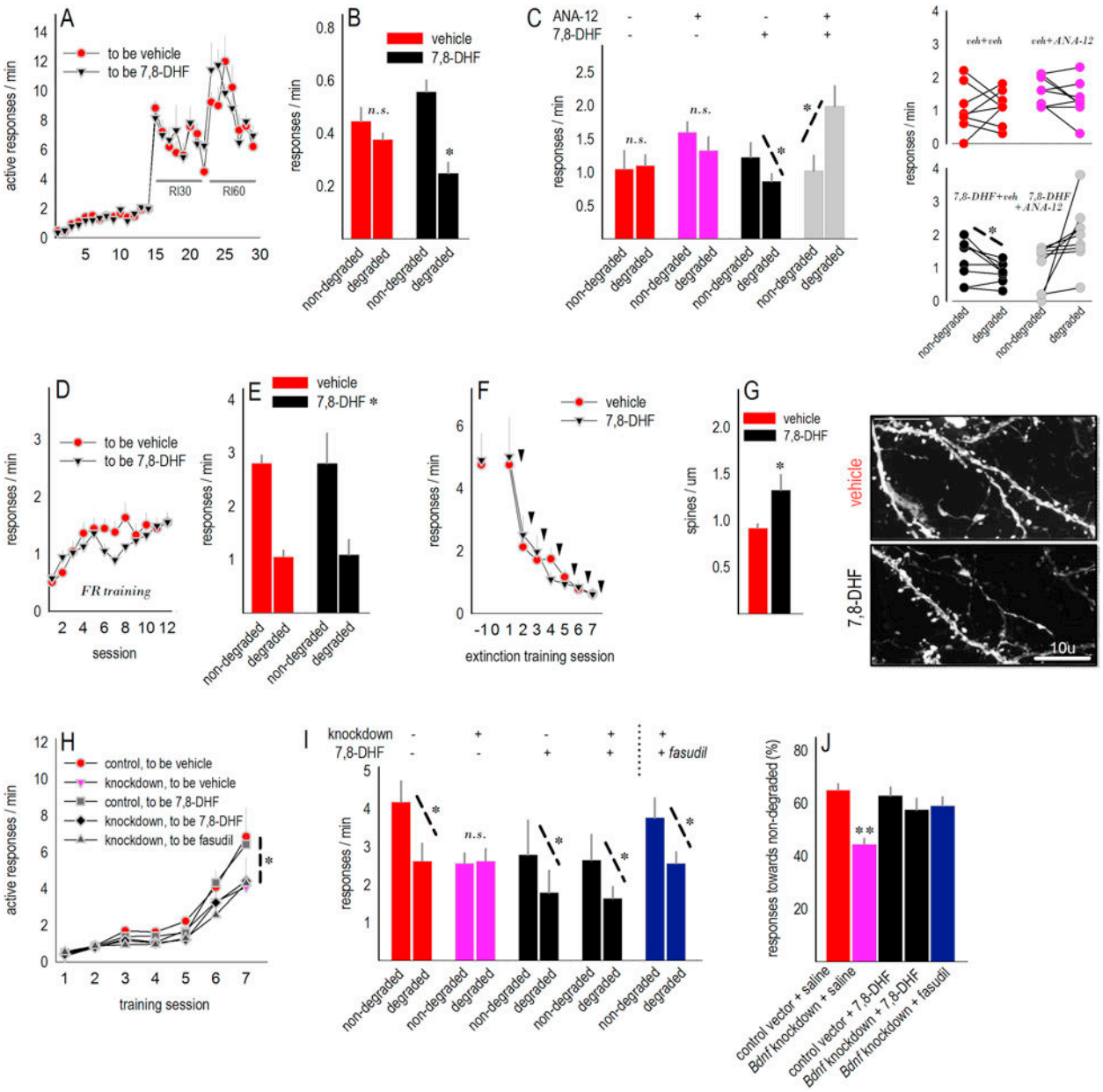

Fig. 6. Rescue of goal-directed decision-making and regulation of VLO dendritic spines

(a) Intact mice were extensively trained to respond for food reinforcement. Escalating random interval schedules are indicated. (b) The TrkB agonist, 7,8-DHF, preserved sensitivity to action-outcome contingency degradation, despite extended response training, while control mice developed habitual response strategies as expected. (c) In a subsequent experiment, pretreatment with the TrkB antagonist, ANA-12, blocked this effect. Group means are represented at left, and individual mice are represented at right. Response acquisition curves for these mice are provided in Suppl. Fig. S1. (d) Separate mice were trained to nose poke using a fixed ratio 1 schedule of reinforcement. (e) 7,8-DHF had no effects when mice would be expected to engage in goal-directed decision-making strategies. (f) Additionally, 7,8-DHF had no effects on extinction conditioning. Each arrow represents

an injection immediately following the test session. (g) Layer V dendritic spines were imaged and enumerated in these mice. 7,8-DHF increased spine density in the VLO. Representative dendritic branches are adjacent. (h) Next, mice with VLO-targeted *Bdnf* knockdown were trained to respond for food reinforcers. (i) *Bdnf* knockdown induced inflexible habit-like responding following instrumental contingency degradation as expected, but 7,8-DHF rescued response selection strategies. Another group of knockdown mice instead received the Rho-kinase inhibitor fasudil, which also rescued goal-directed response strategies. (j) The same data are represented as the percentage of total responses directed towards the intact response-outcome contingency. The pink bar at ~50% indicates that *Bdnf* knockdown mice responded at chance levels, while 7,8-DHF and fasudil restored selective responding. Bars and symbols represent means+SEMs except in c, right. *$p<0.05$ as indicated following *t*-tests, **$p<0.04$ relative to all other groups. “RI” refers to random interval schedules of reinforcement, and “FR” refers to fixed ratio 1 training used throughout.

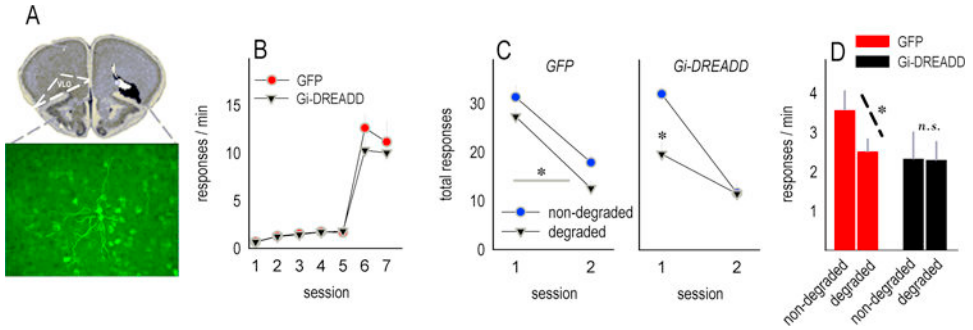

Fig. 7. Gi-DREADD stimulation results in habit-like behavioral inflexibility

(a) Mice were infused bilaterally with AAV-CaMKII-GFP or AAV-CaMKII-hM$_4$D(Gi)-mCitrine. Infusions sites are represented. mCitrine-expressing neurons are shown; the gray box overlaid on the histology image represents the location of these neurons. (b) Response rates did not differ during instrumental response acquisition. (c) When CNO was paired with the degradation of an instrumental contingency, control GFP-expressing mice subsequently preferentially generated the response more likely to be reinforced. Rates are represented in 2×5-min. bins. By contrast, Gi-DREADD-expressing mice initially preferred the 'non-degraded' response, but this goal-directed response strategy decayed. (d) The same findings are represented in bar graph form, again indicating that Gi-DREADD stimulation induced non-selective responding. Symbols and bars represent means+SEMs,*p<0.05.